Pulsed laser-induced nucleation of sodium chlorate at high energy densities

Pulsed laser-induced nucleation of sodium chlorate at high energy densities

Eleanor R. Barber, Nina L. H. Kinney and Andrew J. Alexander*

School of Chemistry, University of Edinburgh, Edinburgh, Scotland, EH9 3JJ

**e-mail: andrew.alexander@ed.ac.uk*

Abstract

We report on a study of laser-induced nucleation (LIN) of sodium chlorate in supersaturated aqueous solutions using focused nanosecond laser pulses at high energy densities (420 kJ cm^{-2}). On irradiation with a single laser pulse, optical breakdown was observed in the form of a luminous plasma, and numerous microbubbles were produced. Based on the observations, we estimate the energy threshold for optical breakdown in the solutions to be 70 J cm^{-2}. Remarkably, even at high energy densities, single laser pulses produced on average only one or two crystals. The mean number of crystals obtained was 1.5 (532 nm) and 1.8 (1064 nm) per sample (3 cm^3). The effect of left circularly polarized (LCP) and right circularly polarized (RCP) light on the nucleation of dextrorotatory (*d*) versus levorotatory (*l*) enantiomorphs of cubic (phase I) sodium chlorate crystals was investigated. No significant correlation between the helicity of circular polarization and the chirality of enantiomorph was observed. The results are consistent with a mechanism involving nucleation of the achiral monoclinic phase III followed by solid–solid transformation to the chiral cubic phase I of sodium chlorate, although this transformation was not observed directly. The use of single-pulse LIN at high pulse energy densities may be useful in exploration of polymorphs, or in production of single crystals for analysis.

1. Introduction

Growth of high-quality crystals is needed for many important applications, such as structure determination by X-ray scattering, or measurement of bulk physical properties. A fundamental challenge in crystallization is to control the balance between the rate of

nucleation versus the rate of crystal growth. For example, the probability of spontaneous nucleation can be increased by raising the supersaturation of a solution; but when supersaturation is too high, it can lead to multiple primary and secondary nucleation events, resulting in small crystallites with poor crystal quality and habit.[1]

To promote crystal growth at low supersaturation, various methods for inducing nucleation by perturbation have been used. Methods include introducing foreign bodies to act as substrates for heterogeneous nucleation, or scratching the internal surface of a glass vessel;[1] these methods are relatively invasive, however. Methods that are less invasive include application of external acoustic waves or electric fields.[2-3] Laser-induced nucleation (LIN) is a promising technique for promoting nucleation which can be applied externally to a closed system.[4-5]

Different optical setups have been used for LIN. The main parameters of the laser light are wavelength, duration of exposure and power density. Garetz, Myerson and co-workers used unfocussed pulsed-nanosecond laser light.[6] Sugiyama, Masuhara and co-workers used tightly focused, continuous-wave (CW) laser light.[5, 7] Both techniques employ laser powers and wavelengths (visible or near-infrared) that avoid photochemical damage to the system, and are therefore commonly known as non-photochemical laser-induced nucleation (NPLIN).[8] At higher laser powers, photochemical and photomechanical processes become important. Femtosecond laser pulses with high peak powers can induce nucleation by cavitation, as studied by Yoshikawa, Matsuhara and co-workers.[9-10] Nucleation by cavitation or pressure waves can also be caused by nanosecond laser pulses with high energy densities, as studied by Soare et al. and Compton and co-workers.[11-13] For all methods of LIN, the mechanisms for nucleation are not fully understood, but it is likely that the different methods share common features.[4]

Sodium chlorate ($NaClO_3$) is an exemplary enantiomorphic material.[14] The most common solid crystal form (form I) at room temperature belongs to a cubic space group ($P2_13$). Cubic sodium chlorate forms left-handed (*l*) and right-handed (*d*) enantiomorphs, which can be distinguished easily by optical rotary dispersion of white light through a pair of crossed polarizers. One advantage to studying sodium chlorate crystallization is the

possibility to distinguish between primary and secondary nucleation processes. An unbiased single primary nucleation event will give a *d* or *l* crystal with equal probability; in contrast, a secondary nucleation event will produce a daughter crystal of the same enantiomorph as the parent seed. Therefore, by counting the ratio of *d* to *l* crystals in a given system, it is sometimes possible to infer the mechanism of nucleation.

The crystallization of sodium chlorate into the two enantiomorphs can be biased by external perturbations.[14] These perturbations can be achiral; for example, rapid stirring of a supersaturated solution leads to spontaneous resolution.[15] The stirring increases the rate of secondary nucleation over primary nucleation so that a single nucleus (*d* or *l*) goes on to dominate the product population of crystals. Another example of achiral perturbation is Viedma ripening, where a random population of crystals can be resolved into all *d* or all *l* by grinding the crystals in contact with saturated solution.[16] Examples of chiral perturbations include seeding, or irradiation with spin-polarized particles, such as β-particles and positrons.[14, 17]

Mirsaleh-Kohan et al. have used focused nanosecond laser pulses to nucleate aqueous supersaturated solutions of simple salts, such as sodium bromate, which is isomorphous with sodium chlorate.[11-12, 18] In their experiments, a sequence of nanosecond laser pulses were focused into the solution or onto the surface of a metallic foil in contact with the solution. Numerous small crystals were formed throughout the solution. Since the foil did not transmit the light, it was concluded that laser-induced shockwaves caused nucleation.

In previous work in our group, we demonstrated NPLIN in molten sodium chlorate, and showed that the samples had a memory of the enantiomorph used to produce the melt.[19-20] Curiously, we had found that aqueous supersaturated sodium chlorate solutions could not be induced to nucleate with unfocussed nanosecond laser pulses. We later attributed this result to the lack of solid nanoparticle impurities in the system, and demonstrated NPLIN after doping solutions with Fe_3O_4 nanoparticles.[21] The nanoparticles absorb light from the nanosecond laser pulses, resulting in localized cavitation events that result in nucleation.[4]

The aim of the present work was to understand more about the mechanism for LIN with nanosecond pulses at high energy densities (~100 kJ cm^{-2}), significantly higher than previous pulsed-laser LIN studies (~1 kJ cm^{-2}).[21-23] We conducted a study on aqueous supersaturated sodium chlorate solutions using single, focused pulses of circularly polarized laser light. We show that that the helicity of light cannot be used to control which enantiomorph of sodium chlorate is nucleated under these conditions. Contrary to expectations, we found that single crystals can be obtained with a single laser pulse, even at these high energy densities. We describe a mechanism based on optical breakdown and cavitation. LIN with single, high-energy laser pulses offers a direct, brute-force route for obtaining single (or few) crystals for solutions that are found to be inactive to conventional NPLIN methods. This method may be employed, for example, in a synthetic laboratory setting where good quality crystals are required for analysis.

2. Experimental methods

Sodium chlorate was purchased from Sigma Aldrich (ReagentPlus, >= 99%) and used without further purification. Ultrapure water (18.2 MΩ cm) was used for preparing solutions. The solubility of sodium chlorate was obtained from fitting the experimental values of Nies and Hulbert,[24] which are similar to the earlier values of Bell.[25] The saturation concentration at 20 °C was 0.955 g $NaClO_3$ per g of H_2O, corresponding to molality C_{sat} = 8.97 mol kg^{-1}. Samples of supersaturated solution ($S = C/C_{sat}$ = 1.21) were prepared from batches of stock solution, and filtered while warm into clean, glass vials through a syringe filter (0.2 μm, cellulose acetate membrane). At this supersaturation, the mole fraction of sodium chlorate in solution was 0.164. Each vial contained approximately 3 cm^3 of solution and was sealed tightly with a screwcap. To achieve supersaturation, the sample vials were heated to approximately 50 °C overnight to dissolve completely, and then cooled slowly to 20 °C (in air, over approximately 2 hours). Samples prepared in this way were found to be metastable for at least 48 hours, and usually substantially longer.

A schematic diagram of the experimental setup is shown in Fig. 1. Laser pulses were delivered from a Nd^{3+}:YAG laser (Surelite II-10) at 532 nm (duration 5.0 ns) and 1064 nm

(duration 6.4 ns). The power was controlled by rotating the axis of a Glan-laser polarizer with respect to the axis of linearly polarized light output from the laser. Circularly polarized light was generated using either a BK7-glass single Fresnel rhomb (at 532 nm) or a quartz multiple-order quarter-wave plate (at 1064 nm) oriented to produce light of known helicity.[26] We define left circular polarization (LCP) and right circular polarization (RCP) in the traditional optics sense, from the point of view of an observer looking into the oncoming beam. For LCP, in a fixed plane as the light passes through, an observer would see the electric field vector rotate anti-clockwise in time. For RCP, the observer would see the electric field vector rotate clockwise. Samples were classified according to the polarization of light used to irradiate the sample.

The mean laser powers for pulse trains at 10 Hz were measured as 0.65 W (532 nm) and 2.6 W (1064 nm). The beam diameter was 8 mm. The equivalent single-shot energy densities before focusing were 130 mJ cm^{-2} (532 nm) and 520 mJ cm^{-2} (1064 nm). In each round of irradiation, a single pulse of laser light was focused into the center of each sample solution using a planoconvex lens with +5 cm focal length. The radius (w_0) of the focal spot was estimated from the following equation,

$$w_0 = \frac{2\lambda f}{\pi D} \qquad (1)$$

where λ is the (vacuum) wavelength, f is the focal length and D is the diameter of the beam before focusing.[27] This gave w_0 values of 2.1 μm (532 nm) and 4.2 μm (1064 nm). We ignore reflections and refraction due to the curvature of the sample vial. The energy densities at the focal point were estimated to be 460 kJ cm^{-2} at both 532 nm and 1064 nm due to the tighter beam waist at the shorter wavelength. Accounting for the pulse duration, the corresponding peak power densities were 87 TW cm^{-2} (532 nm) and 68 TW cm^{-2} (1064 nm). All samples were placed to ensure that the focal volume was well within the solution. The pulse was seen to cause a violent event at the focal point, which caused significant disruption to the solution. No evidence of damage to the vessel walls was observed during or after irradiation. Tests with an in-situ thermocouple showed no

temperature increase during irradiation, within the uncertainty of the measurement (±0.1 °C).

After irradiation, each solution was placed aside and was checked for crystals after 2–4 hours. After this time, any crystals that had formed were removed from the vials and dried. The hand (*d* or *l*) of a crystal enantiomorph was determined by placing it between crossed polarizers and observing the optical rotary dispersion with a white light source.[28] The crystals were sufficiently large (1–4 mm per edge) that this could be achieved without a polarizing microscope. The number of dextrorotatory (*d*) and levorotatory (*l*) crystals was counted for each vial. Samples that produced no crystals were exposed to a further round of irradiation; the maximum number of irradiation rounds used for any sample was 10.

Images of events in square cuvettes made of poly(methyl methacrylate)were taken using a digital camera (Basler ac2040-90um) with macro zoom lens and 532 nm notch filter (Semrock NF01-532U-25). Cuvettes were used only for imaging; otherwise only glass sample vials were used.

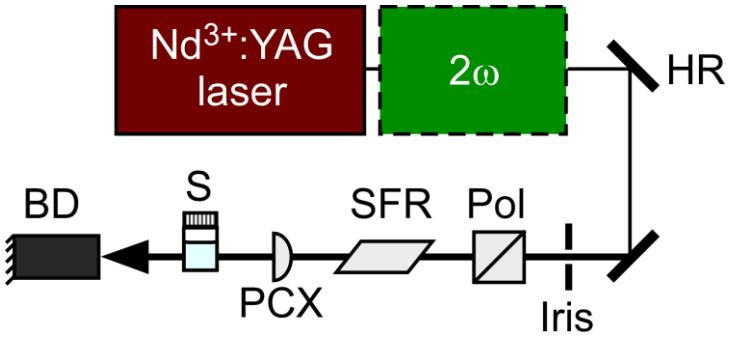

Fig. 1. Schematic diagram of the optical setup used in the present work. HR = high reflection mirror; Iris = adjustable iris; Pol = Glan-laser polarizer; SFR = single Fresnel rhomb (replaced by quarter-wave plate at 1064 nm); PCX = planoconvex lens (+5 cm); S = sample vial containing supersaturated sodium chlorate solution; BD = beam dump. The laser used was a pulsed Nd^{3+}:YAG laser giving light at 1064 nm with optional second-harmonic generator and separation module (2ω) giving 532 nm light.

3. Results

In Fig. 2 we show example images taken during and after the laser pulse strikes the solution in a square cuvette. An example video is given in the Supporting Information

(Video S1). The laser pulse causes a bright optical emission at the focal volume and numerous bubbles, which are seen to move outward. The bright emission is formation of a plasma due to the high energy-density of the laser light. We expect a vapor cavity was formed after the plasma emission, but the time for expansion and collapse (< 1 ms) was too fast for our imaging set-up.[13, 29] The irradiation event was audible as a short, snapping sound, and in many cases the vial could be seen to move from its initial position, unless it was held in place. The audible snapping can be attributed to the release of pressure waves due to the rapid heating and cavitation; the pressure waves are transmitted through the cuvette to the surrounding atmosphere.

The bubbles we see might be composed either from hot water vapor or from gas. Due to immersion in the cold fluid, vapor bubbles would be expected to dissolve rapidly after cooling, on a timescale < 1 ms.[30] Since the bubbles shown in Fig. 2 have survived for at least 0.6 s, we attribute these to gas. The bubbles may come from dissolved gas, or hydrogen and oxygen due to dissociation of the water. The release of bubbles at the bottom of the cuvette suggest that degassing of the solution takes place. Rapid degassing of surrounding solution can be caused by pressure waves and shearing of the solution. It is evident from the rapid transit of the bubbles throughout the volume of the vial that the solution has been violently disrupted.

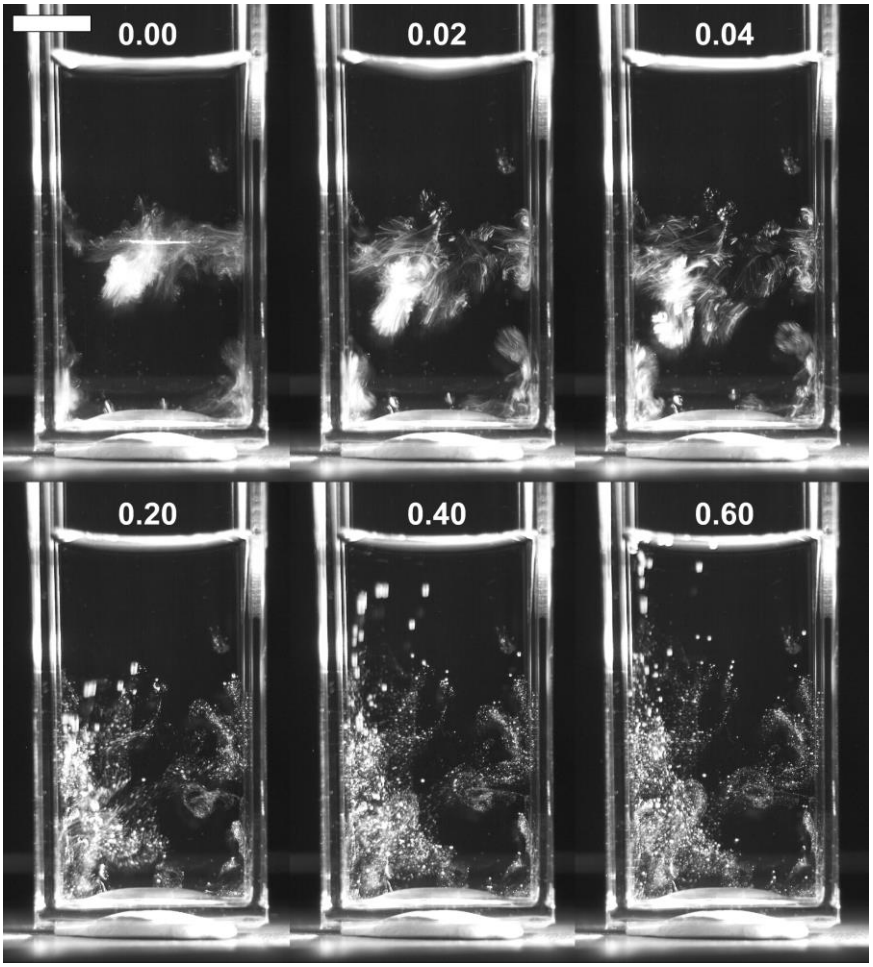

Figure 2. Sequence of images taken during and after a single laser pulse strikes the solution in a cuvette (see Video S1 in the Supporting Information). The scale bar (top left) represents 4 mm. The time (*t*) in seconds is given at the top of each panel. The exposure time for each image was 20 ms. The 532-nm laser pulse travels from left to right in the image. A bright emission due to plasma formation was seen at the center of the solution (the focal volume) at $t = 0$ s, along with release of microbubbles, which move outward and eventually upwards from the focal volume. All of the white objects that can be seen in these images are bubbles; crystals grow slowly and are not visible until approximately 10 minutes after irradiation. The event at $t = 0$ causes release of gas bubbles trapped at the bottom of the cuvette. Note that due to the slow rate of growth, crystals are not visible until approximately 10 mins after nucleation.

Despite the high energy of the irradiation event, we did not see many small crystals as we had expected: in general, only one or two crystals were produced in each vial. After growth, the crystals showed the expected cubic morphology, with edges typically 1–4 mm in length (see Supporting Information, Fig. S2). Fig. 3 shows a summary of the number of

crystals (both *d* and *l*) obtained in the vials. There is no significant preference between LCP and RCP for either laser wavelength. The mean number of crystals obtained was 1.5 (532 nm) and 1.8 (1064 nm).

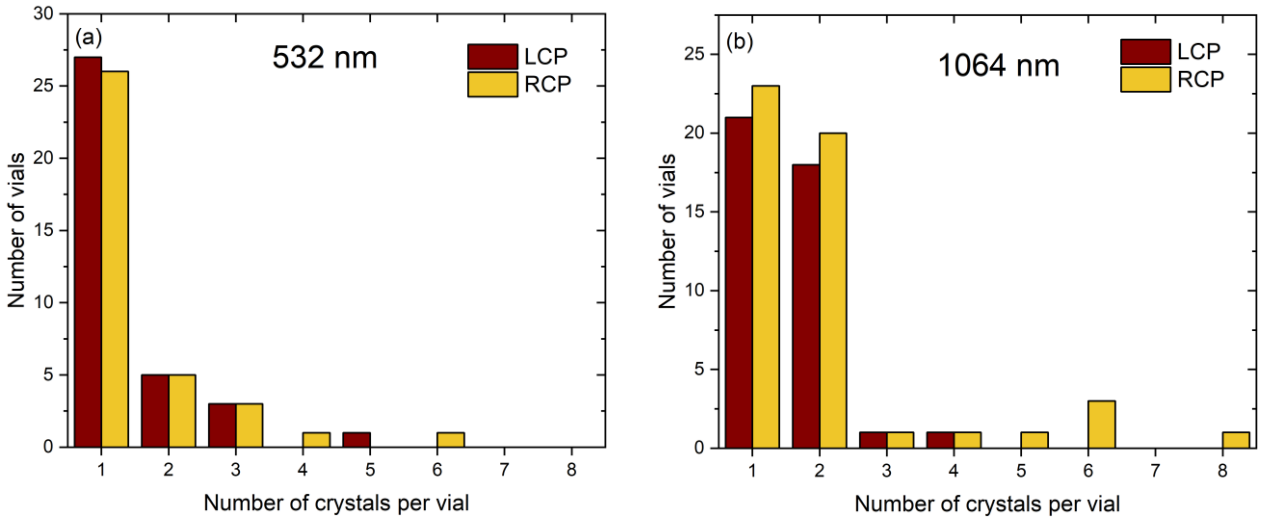

Figure 3. Summary of the total number of $NaClO_3$ crystals (*d* and *l*) obtained per vial using left (LCP) and right (RCP) circularly polarized laser light at (a) 532 nm and (b) 1064 nm. No significant difference between LCP and RCP is observed. The mean number of crystals obtained was 1.5 (532 nm) and 1.8 (1064 nm).

Table 1 presents a summary of the crystals counted after exposure to circularly polarized laser light. N_{vial} is the number of sample vials irradiated, $N_{crystal}$ is the total number of crystals obtained; N_d and N_l are the total numbers of *d* and *l* crystals obtained, respectively. The fraction of dextrorotary crystals was calculated as $F_d = N_d / N_{crystal}$ and the crystal enantiomorphic excess was calculated as cee = $(N_d - N_l) / (N_d + N_l)$. It is clear from the table that there was no systematic correlation between the helicity of the circularly polarized light and the enantiomorph produced.

Wavelength	Polarization	N_{vial}	$N_{crystal}$	N_d	N_l	F_d	cee
532 nm	LCP	36	51	27	24	0.53 ± 0.07	0.06 ± 0.15
	RCP	36	55	24	31	0.44 ± 0.06	–0.13 ± 0.12
1064 nm	LCP	41	64	30	34	0.47 ± 0.05	–0.06 ± 0.10
	RCP	50	101	48	53	0.48 ± 0.04	–0.05 ± 0.08

Table 1. Summary of the results obtained for nucleation of sodium chlorate solutions with left (LCP) or right (RCP) circularly polarized light. N_{vial} is the number of sample vials irradiated, $N_{crystal}$ is the total number of crystals obtained; N_d and N_l are the total numbers of *d* and *l* crystals obtained, respectively. F_d is the fraction of dextrorotary crystals and cee is the crystal enantiomorphic excess (see text for details). The uncertainties quoted are single standard deviations of the sample, weighted by the number of crystals in each vial.[28]

4. Discussion

When an intense, focused laser pulse interacts with a liquid such as water, various processes take place that result in optical breakdown and cavitation.[31] Early in the time duration of the pulse, multiphoton ionization and field ionization take place, producing quasi-free electrons. Once produced, a free electron absorbs more photons, increasing its kinetic energy. A free electron with sufficiently high kinetic energy can cause impact ionization, producing an additional free electron, and this sequence of events can amplify, leading to so-called avalanche ionization or cascade ionization. Eventually a critical free-electron density is attained, and the resulting plasma can be luminescent, as seen in Fig. 2. The fast, localized deposition of energy leads to production of a cavity in the liquid, due to both the rapid increase in temperature and emission of a pressure wave. Within the focal volume, electron-induced processes, such as dissociative ionization, and other chemical reactions can occur. In the case of water for example, this leads to production of H_2 and O_2 gas.

In a general comparison, femtosecond laser pulses tend to have relatively low energy and high peak power, whereas nanosecond pulses have low peak power and high energy. The balance between the various electron processes outlined above depends on the pulse duration and focusing conditions, e.g., numerical aperture (NA), but the net result

is optical breakdown and cavitation.[31] Some previous studies have used focused laser pulses to induce crystallization.[10-13, 18, 29, 32] Results for both femtosecond and nanosecond pulses suggest that the formation and collapse of a cavity is key to nucleation of a solid from a metastable liquid.

Soare et al. studied nucleation of ammonium sulfate using nanosecond laser pulses (~5 kJ cm^{-2}) focused into a gap (~50 μm) between two glass windows.[13] After irradiation they observed a ring of 10–30 crystals growing around the focal region on one of the windows. Lindinger et al. studied nucleation of ice with nanosecond laser pulses (~6 kJ cm^{-2}) using high-speed imaging.[29] They saw optical breakdown followed by cavitation and production of gas microbubbles: ice nucleation was observed only at these bubbles. Pre-existing microbubbles, from previous laser pulses, were particularly prone to ice nucleation if they were sufficiently close to the cavitation event. Yoshikawa et al. and Iefuji et al. used femtosecond pulses (~0.05 kJ cm^{-2}) to nucleate proteins in gel and in solution.[10, 32] Fast imaging suggested that the expansion and collapse of the cavitation bubble forms a halo of concentrated solute.[32]

Compton and co-workers described shock-wave crystallization using nanosecond laser pulses (~20 kJ cm^{-2}) focused either directly into solution, or onto a thin steel plate floating on top of a solution.[11-12, 18] Numerous small crystals were observed throughout the solution, or raining down from the plate, respectively. They saw many more crystals than in the present work, and we attribute this to the use of multiple laser pulses. Successive pulses create further primary nucleation events and promote secondary nucleation by shear and mixing, producing many more crystals. Efficient absorption of the laser pulses will also increase production of crystals. In the case of the steel plate floating on the solution, the laser light will be absorbed very efficiently by the metal surface. One area for future study would be to look for evidence of cavitation on the solution side of the plate.

Experiments have shown that the energy threshold (E_{th}) for optical breakdown in water is approximately half the value at 532 nm compared to 1064 nm.[33] From the moving-breakdown model of Docchio et al.,[34] we can estimate the breakdown threshold from the observed length (z_{max}) of the plasma, as follows:

$$z_{max} = z_0\sqrt{\beta - 1} \quad (2)$$

where $z_0 = n\pi w_0^2/\lambda$ is the Rayleigh range and $\beta = E / E_{th}$ is the dimensionless pulse energy. We estimate the refractive index of the sodium chlorate solution to be n = 1.40. At 532 nm, the focal radius w_0 = 2.1 μm (Eq. 1) and we calculate z_0 = 37 μm. From the image (Fig. 2 at 0.0 s) we measure the breakdown length as $z_{max} \approx$ 3.0 mm. Thus, we obtain β = 6600 and E_{th} = 70 J cm^{-2}. These values indicate that the pulse energies we used were four orders of magnitude above the threshold for optical breakdown. The value for E_{th} is lower than that previously measured for pure water (174 J cm^{-2}) which we attribute to a lower ionization threshold for the sodium chlorate solution.[33] We saw on average only slightly more crystals per vial at 1064 nm than 532 nm, but the reason for this is not clear. One reason may be that the focal volume at 1064 nm is a factor of 8 larger than at 532 nm (Eqs 1 and 2). The absorption coefficient of water at 1064 nm is 350 times larger than at 532 nm,[35] so it seems unlikely that the difference in linear absorption is the reason.

Fig. 2 demonstrates that a large amount of energy was dispersed into the solution from only a single laser pulse. Given the supersaturation (S = 1.21) and high energy density (460 kJ cm^{-2}) used, it is remarkable that on average only one or two crystals were formed per vial. This indicates that secondary nucleation was not significant. One explanation for the low number of crystals is that the primary nucleation events are very selective and localized, and that the low rate of mixing means that secondary nucleation does not occur.

We saw no significant correlation between circular polarization and the enantiomorph produced (Table 1). This is consistent with a nucleation mechanism that results from thermomechanical cavitation due to the optical pulse. The equal numbers of *d* or *l* crystals could indicate random nucleation of the chiral phase I of sodium chlorate. Based on the low numbers of crystals produced, however, we propose that crystallization takes place by nucleation first of the achiral phase III of sodium chlorate, followed by solid–solid transformation from phase III to I, resulting in random formation of either *d* or *l* crystals. Our proposed mechanism is based on observations of crystallization made previously in our group for molten $NaClO_3$, and by Niinomi et al. for aqueous solutions.[20, 36] The solid transformation of $NaClO_3$ from the monoclinic phase III to cubic phase I involves

a coordinated sliding of crystal layers. It may also involve another intermediate phase (phase II) which contains equal numbers of left-handed and right-handed sodium-ion octahedra.[37-38] The pathway to either the *d* or *l* enantiomorph should be equivalent energetically, and hence equal numbers of the enantiomorphs should result.

In previous work, we found that the statistics of crystal samples, obtained by cooling from the melt while stirring, could only be rationalized by invoking nucleation of an achiral phase.[20] Optical microscopy experiments by Niinomi et al. on evaporating microdroplets of sodium chlorate solution, revealed that the achiral phase III of sodium chlorate forms first, and later transforms to phase I, apparently following Ostwald's rule of stages.[36, 38] Niinomi et al. showed that nucleation can be promoted by using absorption of CW laser light at high powers, or by excitation of plasmon resonances in Ag nanoparticles or nanolattices.[39-42] Reviewing all the evidence currently available for this system leads us to conclude that primary nucleation of $NaClO_3$ directly to the chiral phase I is at least hindered, or indeed might not occur at all, i.e., that spontaneous ambient crystallizations of $NaClO_3$ involve phase III.

If we accept that nucleation of phase I is hindered, nucleation of phase III can explain the selectivity in the present work. Below the melting point of $NaClO_3$ at 262 °C, the Gibbs free energy of phase III is higher than phase I.[43] Solubility measurements at room temperature show the saturation concentration of phase III is about 1.6 times higher than phase I.[44] This would place a greater constraint on the concentration required for nucleation, making the process more selective and localized. We consider that the optical breakdown, followed by formation of a cavity, can produce a locally higher supersaturation that is sufficiently high to form phase III. Recent computational fluid-flow simulations by Hidman et al. support the idea of formation of a concentrated fluid region at the periphery of a laser-induced vapor cavity.[30] Our proposed mechanism is consistent with both the observed selective formation of only a few crystals per sample, and the lack of preference for the enantiomorph of phase I crystals.

5. Conclusions

In summary, we have conducted a study of laser-induced nucleation (LIN) using single nanosecond laser pulses focused into bulk samples of supersaturated aqueous sodium chlorate. The pulse energy densities employed were significantly higher than previous studies of LIN, and many orders of magnitude higher than the estimated threshold for optical breakdown. We observed optical breakdown, formation of a luminescent plasma, and a violent release of persistent bubbles throughout the solution. Remarkably, despite the large amount of energy deposited, we found only one or two crystals were formed on average per sample. We did not see any correlation between the helicity of circularly polarized light used, and the resulting enantiomorph (dextrorotary or levorotary) of the cubic chiral phase (phase I) of sodium chlorate. These observations indicate that secondary nucleation was not significant, and that the primary nucleation events induced by the laser were highly localized and selective. Our observations are consistent with a mechanism for crystallization via nucleation of the achiral phase III of sodium chlorate. This mechanism requires transiently high supersaturations caused by the rapid formation and collapse of a cavity in the solution following optical breakdown. Our results suggest that LIN with single high-energy pulses may be useful in exploration for new polymorphs, or in production of crystals for analysis.

Associated Content

Supporting Information

The Supporting Information is available free of charge on the ACS Publications website at DOI: 10.1021/acs.cgd.xxxxxx.

(1) Video showing a single laser pulse irradiated onto a cuvette containing the supersaturated sodium chlorate solution; (2) Image of sodium chlorate crystals 120 min after irradiation by a single laser pulse.

Author Information

Corresponding Author

*E-mail: andrew.alexander@ed.ac.uk

ORCID

Andrew J. Alexander: 0000-0002-0897-020X

Notes

The authors declare no competing financial interest.

Acknowledgements

We are grateful to the Engineering and Physical Sciences Research Council (EPSRC EP/L022397/1) and to the CMAC Future Manufacturing Research Hub (http://www.cmac.ac.uk) for supporting this work. Data employed in this study are available via the Edinburgh DataShare repository (DOI:10.7488/ds/2632).

References

1. Mullin, J. W., *Crystallization*. 4th ed.; Butterworth-Heinemann: Oxford, 2001.

2. Nalesso, S.; Bussemaker, M. J.; Sear, R. P.; Hodnett, M.; Lee, J. A review on possible mechanisms of sonocrystallisation in solution. *Ultrason. Sonochem.* **2019,** *57*, 125-138.

3. Aber, J. E.; Arnold, S.; Garetz, B. A.; Myerson, A. S. Strong dc electric field applied to supersaturated aqueous glycine solution induces nucleation of the gamma polymorph. *Phys. Rev. Lett.* **2005,** *94*, 145503.

4. Alexander, A. J.; Camp, P. J. Non-photochemical laser-induced nucleation. *J. Chem. Phys.* **2019,** *150*, 040901.

5. Sugiyama, T.; Adachi, T.; Masuhara, H. Crystallization of Glycine by Photon Pressure of a Focused CW Laser Beam. *Chem. Lett.* **2007,** *36*, 1480-1481.

6. Garetz, B. A.; Aber, J. E.; Goddard, N. L.; Young, R. G.; Myerson, A. S. Nonphotochemical, polarization-dependent, laser-induced nucleation in supersaturated aqueous urea solutions. *Phys. Rev. Lett.* **1996,** *77*, 3475-3476.

7. Rungsimanon, T.; Yuyama, K.; Sugiyama, T.; Masuhara, H. Crystallization in Unsaturated Glycine/D2O Solution Achieved by Irradiating a Focused Continuous Wave Near Infrared Laser. *Cryst. Growth. Des.* **2010,** *10*, 4686-4688.

8. Clair, B.; Ikni, A.; Li, W.; Scouflaire, P.; Quemener, V.; Spasojevic-de Bire, A. A new experimental setup for high-throughput controlled non-photochemical laser-induced nucleation: application to glycine crystallization. *J. Appl. Crystallogr.* **2014,** *47*, 1252-1260.

9. Adachi, H.; Takano, K.; Hosokawa, Y.; Inoue, T.; Mori, Y.; Matsumura, H.; Yoshimura, M.; Tsunaka, Y.; Morikawa, M.; Kanaya, S.; Masuhara, H.; Kai, Y.; Sasaki, T. Laser irradiated growth of protein crystal. *Jap. J. Appl. Phys.* **2003,** *42*, L798-L800.

10. Yoshikawa, H. Y.; Murai, R.; Sugiyama, S.; Sazaki, G.; Kitatani, T.; Takahashi, Y.; Adachi, H.; Matsumura, H.; Murakami, S.; Inoue, T.; Takano, K.; Mori, Y. Femtosecond laser-induced nucleation of protein in agarose gel. *J. Cryst. Growth* **2009,** *311*, 956-959.

11. Fisher, A.; Pagni, R. M.; Compton, R. N.; Kondepudi, D., Laser Induced Crystallization. In *Nanoclusters: A Bridge across Disciplines*, Jena, P.; Castleman, A. W., Eds. Elsevier: Amsterdam, The Netherlands, 2010.

12. Mirsaleh-Kohan, N.; Fischer, A.; Graves, B.; Bolorizadeh, M.; Kondepudi, D.; Compton, R. N. Laser Shock Wave Induced Crystallization. *Cryst. Growth. Des.* **2017,** *17*, 576-581.

13. Soare, A.; Dijkink, R.; Pascual, M. R.; Sun, C.; Cains, P. W.; Lohse, D.; Stankiewicz, A. I.; Kramer, H. J. M. Crystal Nucleation by Laser-Induced Cavitation. *Cryst. Growth. Des.* **2011,** *11*, 2311-2316.

14. Pagni, R. M.; Compton, R. N. Asymmetric Synthesis of Optically Active Sodium Chlorate and Bromate Crystals. *Cryst. Growth. Des.* **2002,** *2*, 249-253.

15. Kondepudi, D. K.; Kaufman, R. J.; Singh, N. Chiral symmetry-breaking in sodium-chlorate crystallization. *Science* **1990,** *250*, 975-976.

16. Viedma, C. Chiral Symmetry Breaking During Crystallization: Complete Chiral Purity Induced by Nonlinear Autocatalysis and Recycling. *Phys. Rev. Lett.* **2005,** *94*, 065504.

17. Mahurin, S.; McGinnis, M.; Bogard, J. S.; Hulett, L. D.; Pagni, R. M.; Compton, R. N. Effect of beta radiation on the crystallization. of sodium chlorate from water: A new type of asymmetric synthesis. *Chirality* **2001,** *13*, 636-640.

18. Fischer, A. T. PhD thesis. University of Tennessee, Knoxville, 2006.

19. Ward, M. R.; Copeland, G. W.; Alexander, A. J. Chiral hide-and-seek: Retention of enantiomorphism in laser-induced nucleation of molten sodium chlorate. *J. Chem. Phys.* **2011,** *135*, 114508.

20. Ward, M. R.; Copeland, G. W.; Alexander, A. J. Enantiomorphic symmetry breaking in crystallization of molten sodium chlorate. *Chem. Comm.* **2010,** *46*, 7634-7636.

21. Ward, M. R.; Mackenzie, A. M.; Alexander, A. J. Role of Impurity Nanoparticles in Laser-Induced Nucleation of Ammonium Chloride. *Cryst. Growth. Des.* **2016,** *16*, 6790-6796.

22. Liu, Y.; van den Berg, M. H.; Alexander, A. J. Supersaturation dependence of glycine polymorphism using laser-induced nucleation, sonocrystallization and nucleation by mechanical shock. *PCCP* **2017,** *19*, 19386-19392.

23. Kacker, R.; Dhingra, S.; Irimia, D.; Ghatkesar, M. K.; Stankiewicz, A.; Kramer, H. J. M.; Eral, H. B. Multiparameter Investigation of Laser-Induced Nucleation of Supersaturated Aqueous KCl Solutions. *Cryst. Growth. Des.* **2018,** *18*, 312-317.

24. Nies, N. P.; Hulbert, R. W. Solubility isotherms and specific gravities in the sodium metaborate-sodium chlorate-water system. *J. Chem. Eng. Data* **1969,** *14*, 14-16.

25. Bell, H. C. Solubility of Sodium Chlorate. *J. Chem. Soc.* **1923,** *123*, 2713-2714.

26. Alexander, A. J. Determination of the helicity of oriented photofragments. *J. Chem. Phys.* **2005,** *123*, 194312.

27. Siegman, A. E., *Lasers*. University Science Books: Sausalito, CA, USA, 1986.

28. Alexander, A. J. Crystallization of Sodium Chlorate with d-Glucose Co-Solute Is Not Enantioselective. *Cryst. Growth. Des.* **2008,** *8*, 2630-2632.

29. Lindinger, B.; Mettin, R.; Chow, R.; Lauterborn, W. Ice Crystallization Induced by Optical Breakdown. *Phys. Rev. Lett.* **2007,** *99*, 045701.

30. Hidman, N.; Sardina, G.; Maggiolo, D.; Ström, H.; Sasic, S. Laser-induced vapour bubble as a means for crystal nucleation in supersaturated solutions—Formulation of a numerical framework. *Experimental and Computational Multiphase Flow* **2019,** *1*, 242-254.

31. Vogel, A.; Noack, J.; Hüttman, G.; Paltauf, G. Mechanisms of femtosecond laser nanosurgery of cells and tissues. *Appl. Phys. B* **2005,** *81*, 1015-1047.

32. Iefuji, N.; Murai, R.; Maruyama, M.; Takahashi, Y.; Sugiyama, S.; Adachi, H.; Matsumura, H.; Murakami, S.; Inoue, T.; Mori, Y.; Koga, Y.; Takano, K.; Kanaya, S. Laser-induced nucleation in protein crystallization: Local increase in protein concentration induced by femtosecond laser irradiation. *J. Cryst. Growth* **2011,** *318*, 741-744.

33. Vogel, A.; Nahen, K.; Theisen, D.; Noack, J. Plasma formation in water by picosecond and nanosecond Nd:YAG laser pulses. I. Optical breakdown at threshold and superthreshold irradiance. *IEEE J. Sel. Top. Quantum Electron.* **1996,** *2*, 847-860.

34. Docchio, F.; Regondi, P.; Capon, M. R. C.; Mellerio, J. Study of the temporal and spatial dynamics of plasmas induced in liquids by nanosecond Nd:YAG laser pulses. 1: Analysis of the plasma starting times. *Appl. Opt.* **1988,** *27*, 3661-3668.

35. Hale, G. M.; Querry, M. R. Optical Constants of Water in the 200-nm to 200-µm Wavelength Region. *Appl. Opt.* **1973,** *12*, 555-563.

36. Niinomi, H.; Yamazaki, T.; Harada, S.; Ujihara, T.; Miura, H.; Kimura, Y.; Kuribayashi, T.; Uwaha, M.; Tsukamoto, K. Achiral Metastable Crystals of Sodium Chlorate Forming Prior to Chiral Crystals in Solution Growth. *Cryst. Growth. Des.* **2013,** *13*, 5188-5192.

37. Meyer, P.; Rimsky, A. Méchanism de la Transition d'une Phase Métastable vers la Phase Stable pour le Chlorate de Sodium. *Acta Cryst.* **1979,** *A35*, 871-876.

38. Niinomi, H.; Miura, H.; Kimura, Y.; Uwaha, M.; Katsuno, H.; Harada, S.; Ujihara, T.; Tsukamoto, K. Emergence and Amplification of Chirality via Achiral–Chiral Polymorphic Transformation in Sodium Chlorate Solution Growth. *Cryst. Growth. Des.* **2014,** *14*, 3596-3602.

39. Niinomi, H.; Sugiyama, T.; Miyamoto, K.; Omatsu, T. "Freezing" of NaClO3 Metastable Crystalline State by Optical Trapping in Unsaturated Microdroplet. *Cryst. Growth. Des.* **2018,** *18*, 734-741.

40. Niinomi, H.; Sugiyama, T.; Tagawa, M.; Murayama, K.; Harada, S.; Ujihara, T. Enantioselective amplification on circularly polarized laser-induced chiral nucleation from a NaClO3 solution containing Ag nanoparticles. *CrystEngComm* **2016,** *18*, 7441-7448.

41. Niinomi, H.; Sugiyama, T.; Tagawa, M.; Maruyama, M.; Ujihara, T.; Omatsu, T.; Mori, Y. Plasmonic Heating-Assisted Laser-Induced Crystallization from a NaClO3 Unsaturated Mother Solution. *Cryst. Growth. Des.* **2017,** *17*, 809-818.

42. Niinomi, H.; Sugiyama, T.; Tagawa, M.; Harada, S.; Ujihara, T.; Uda, S.; Miyamoto, K.; Omatsu, T. In Situ Observation of Chiral Symmetry Breaking in NaClO3 Chiral Crystallization Realized by Thermoplasmonic Micro-Stirring. *Cryst. Growth. Des.* **2018,** *18*, 4230-4239.

43. Meyer, P. Polymorphisme du chlorate de sodium. *C. R. Seances Acad. Sci., Ser. C* **1972,** *274*, 843-845.

44. Niinomi, H.; Horio, A.; Harada, S.; Ujihara, T.; Miura, H.; Kimura, Y.; Tsukamoto, K. Solubility measurement of a metastable achiral crystal of sodium chlorate in solution growth. *J. Cryst. Growth* **2014,** *394*, 106-111.

For Table of Contents Use Only

Pulsed laser-induced nucleation of sodium chlorate at high energy densities

Eleanor R. Barber, Nina L. H. Kinney and Andrew J. Alexander

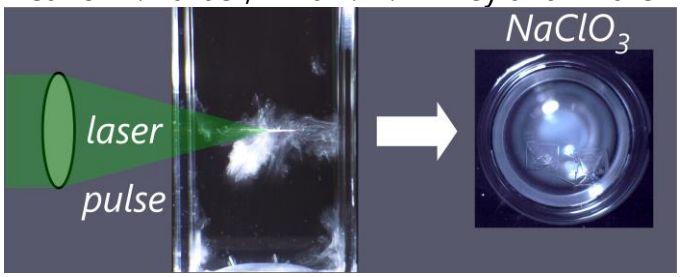

Synopsis

Single pulses of focussed, nanosecond laser light cause nucleation of a few crystals of sodium chlorate in supersaturated solutions. The method may be useful in exploration for new polymorphs, or in production of single crystals for analysis.